

Article

Fibrochondrocyte Growth and Functionality on TiO₂ Nanothin Films

Sharon Ronald ¹ and David K. Mills ^{2,3,*}

¹ University of Texas Medical Branch, John Sealy Hospital, Galveston, TX 77555, USA; ronald.sharon@gmail.com

² Center for Biomedical Engineering and Rehabilitation Science, Louisiana Tech University, Ruston, LA 71272, USA

³ School of Biological Sciences, Louisiana Tech University, Ruston, LA 71272, USA

* Correspondence: dkmills@latech.edu; Tel.: +1-318-257-2640

Academic Editor: Francesco Puoci

Received: 17 March 2016; Accepted: 7 June 2016; Published: 15 June 2016

Abstract: Disorders affecting the temporomandibular joint (TMJ) are a long-standing health concern. TMJ disorders (TMJD) are often associated with an internal disc derangement accompanied by a suite of symptoms including joint noises, jaw dysfunction, and severe pain. The severity of patient symptoms and their reoccurrence can be alleviated to some extent with conservative therapy; however, refractory cases often require surgery that has shown only limited success. Bioengineered scaffolds with cell supportive surfaces and nanoarchitectures that mimic TMJ tissue structure may offer an alternative treatment modality. In this study, titanium dioxide (TiO₂) nanothin films, fabricated by layer-by-layer assembly, were examined as means for creating such a scaffold. The viability and growth of TMJ discal fibrochondrocytes (FCs) were assessed through MTT and DNA assays and total protein content over a 14-day experimental period. ELISA was also used to measure expression of types I and II collagen, decorin and aggrecan. Quantitative analyses demonstrated that FCs synthesized characteristic discal matrix proteins, with an increased production of type I collagen and decorin as opposed to collagen type II and aggrecan. A stimulatory effect on discal FC proliferation and extracellular matrix (ECM) expression with thicker nanofilms was also observed. The cumulative results suggest that TiO₂ nanofilms may have potential as a TMJ scaffolding material.

Keywords: fibrochondrocytes; functionality; nanoassembly; substrate; titanium dioxide

1. Introduction

The temporomandibular joint (TMJ) disc is an elastic fibrocartilagenous tissue located between the head of the mandibular condyle and the squamous portion of the temporal bone [1–3]. The disc functions as an integral component of the TMJ and aids in joint lubrication, cushions and absorbs shock, and promotes smoothness of movement between the articulating surfaces [3–5]. Fibrochondrocytes and fibroblasts are the two cell types found within the disc [2,4,6,7]. Fibrochondrocytes predominate within the disc itself, and fibroblasts are more numerous in the attachment tissues and the junction of the disc with surrounding tissues [6–8]. The disc consists of an extensive extracellular matrix (ECM) with type I collagenous fiber bundles predominating [2,4–6]. Interspersed between the collagenous fiber bundles are elastic and type II collagen fibers and the proteoglycans aggrecan and decorin [1,2,7–11].

Soft tissue remodeling or degenerative changes due to derangements of the TMJ disc can impair normal joint function and cause acute or chronic pain symptoms. Surgeries, including discectomy, eminectomy, condylotomy or, procedures involving repositioning of the disc such as disc/condylar plication, discal suturing or a combination of different surgical procedures, is usually suggested as a permanent treatment option in alleviating TMJ disorders' (TMJD) symptoms [12–14]. However, such

treatment modalities often involve significant post-surgical complications and have demonstrated limited successes in treating TMJD often requiring revision surgery [5,10,12]. As TMJD patients have limited treatment options [15,16], the development of a functional bioengineered TMJ repair tissue becomes a critical need [17,18]. The essence of bioengineering discal tissues lies in the choice of a viable biomaterial that supports cell adhesion, growth and functionality leading to the formation of a new tissue [19–21]. The emphasis in the bioengineering of many soft and hard tissues has been placed on scaffolds with a modified surface that enhance cellular interactions with the scaffold's surface [22–25]. Diverse surface modification techniques, thermal deposition, chemical self-assembly, microfabrication, physisorption, plasma spraying, particle blasting, and acid etching, have been developed [26,27]. However, these techniques pose some problems including intrinsic defects, uneven deposition and poor film adhesion, instability, microcracks and manufacturing difficulties [26–28].

One method that may hold potential for TMJ bioengineering is layer-by-layer (LBL) nanoassembly. LBL nanoassembly is based on the principle of electrostatic attraction between oppositely charged particles [28,29]. LBL nanoassembly is a versatile technique and offers promise as a potential fabrication method for modifying scaffolds and implant surfaces. LBL scaffolds retain the biological activity of biomolecules adsorbed/embedded within the film and facilitate increased cell phenotype retention, cell growth and directed differentiation [30–34]. Also, LBL technique offers manufacturing feasibility in modifying specific features of the scaffolds such as stiffness, topography, and surface chemistry, suitable for its use as an implant scaffold or as a drug delivery system [22,28,29].

The current study assessed the potential of LBL assembled TiO₂ nanofilms as a potential scaffold or surface coating material for repairing damaged TMJ tissues. Cell viability, growth and functionality of TMJ fibrochondrocytes on TiO₂ nanosubstrates were studied. The effects of increasing TiO₂ bilayers on FC response were also examined. Fibrochondrocytes proliferated and produced an abundant ECM on all nanofilms with a marked increase observed in FC functionality on thicker TiO₂ nanofilms. This study suggests TiO₂ nanofilms may hold potential as a method for producing materials for the repair of damaged or diseased TMJ tissues.

2. Results

2.1. Cytotoxicity Assays

The current study aimed to quantitatively analyze FC proliferation and functionality with increased TiO₂ surface coatings. Prior to proceeding to the quantitative assays, FC adherence and cytocompatibility on TiO₂ nanosubstrates with increasing thickness was tested. Phase contrast observations showed TMJ fibrochondrocytes attached easily to the TiO₂ surfaces and spread across the nanosubstrates as seen in Figure 1A. Many cells displayed the oval or polygonal cell morphology of typical fibrochondrocytes. Live Dead assays confirmed these observations and showed that the cells on the substrates thrived and increased in cell density over the experimental period (Figure 1B–D) with the expected result that TiO₂ nanosubstrates provided a cytocompatible, cell adherent surface supporting FC phenotype stability.

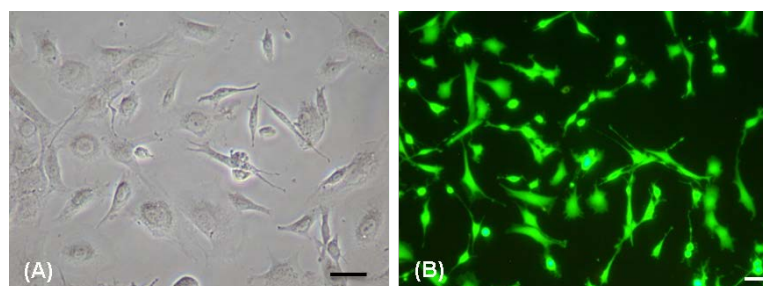


Figure 1. Cont.

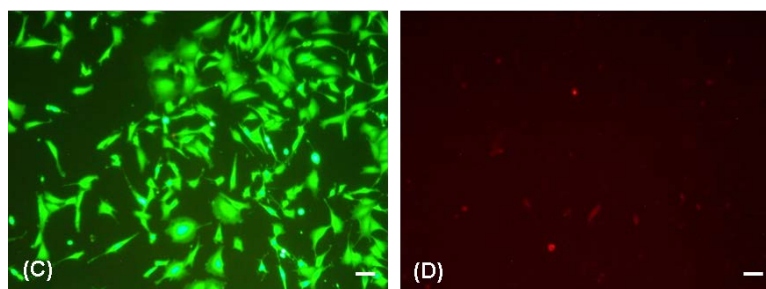


Figure 1. Cell culture on 5 and 10 layered TiO₂ nanosubstrates at culture days 7 and 14. Scale bar = 10 μm. (A) Phase contrast microscopic image indicates FC adherence and proliferation at culture day 7 on 5 layered TiO₂ nanosubstrate; Typical FC morphology (oval and polygonal) observed on the nanosubstrate (B–D) indicate Live Dead Assay images. The green fluorescent dye (Live Dye™) indicates viable FC cell culture and the red fluorescent (propidium iodide) indicates dead cells. (B) Indicates FCs at culture day 7 on 5 layered TiO₂ nanosubstrate. (C) And (D) indicates FCs at culture day 14 10 layered TiO₂ nanosubstrate.

2.2. Proliferation Assays

2.2.1. MTT Proliferation Assay

An increased rate of FC proliferation was observed with increased days in culture and for all the substrates (Figure 2). Enhanced proliferation was seen on culture day 14 compared to culture day 7 for all substrates. An increased number of proliferating cells occurred on TiO₂ nanosubstrates as compared to control substrates. An increase in the number of TiO₂ nanolayers deposited on the LBL scaffolds was observed to be a potential factor in promoting cellular growth. Statistical analyses conducted on the MTT results demonstrated that FC proliferation was statistically significant ($p < 0.05$) with an increase in culture days and with increasing nanothin film thickness.

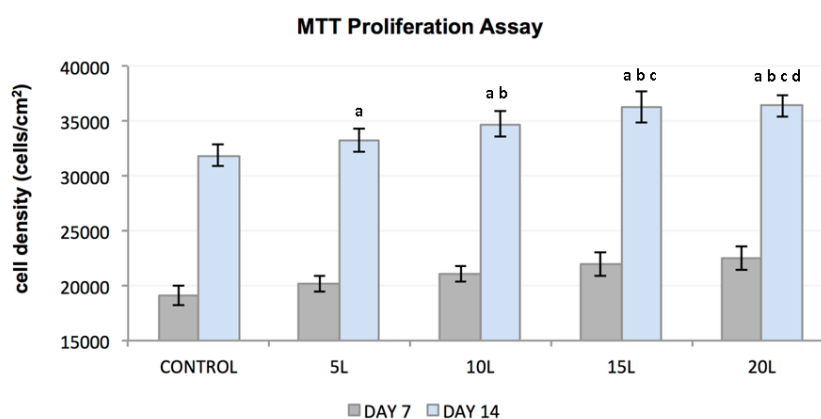


Figure 2. Plot represents FC cell density (y -axis) as a function of control substrates and increasing nanolayers of TiO₂ nanosubstrates (x -axis) at 7 and 14 culture days. All data are shown as mean \pm standard deviation, with a sample size of 6 for all substrates. Substrates represented by letters different (a, b, c, d) are considered statistically significant ($p < 0.05$), using two-way analysis of variance. “a” indicates nanosubstrates that show statistically significant cell numbers w.r.t control substrates. “b”, “c” and “d” indicates nanosubstrates that show statistically significant cell numbers w.r.t 5 L, 10 L and 15 L nanosubstrates respectively.

2.2.2. DNA Quantitation Assay

The DNA quantitation assay substantiated the results obtained from the MTT proliferation assay (Figure 3a,b). FC response was evaluated for a culture period of 3, 7, 10 and 14 days for an accurate

assessment of FC proliferative rate. FC proliferation increased over a period of 14 days and with increasing TiO₂ nanofilms, although enhanced proliferation on the nanosubstrates was not observed from the control substrates. Statistical analyses on the DNA Quantitation results corroborated with the MTT results demonstrating statistically significant ($p < 0.05$) FC proliferation with increasing culture days, day 14 as compared to day 7, and with increasing nanolayers.

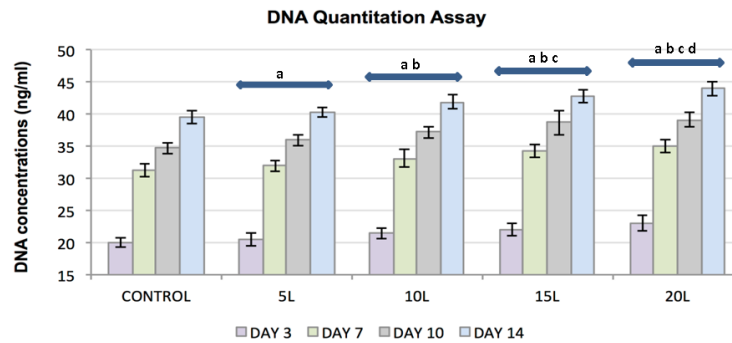


Figure 3. Plot represents DNA concentration of FC lysate samples (*y*-axis) as a function of control substrates and increasing nanolayers of TiO₂ nanosubstrates (*x*-axis) at 3, 7, 10 and 14 culture days. All data are shown as mean ± standard deviation, with a sample size of 6 for all substrates. Substrates represented by letters different (a, b, c, d) are considered statistically significant ($p < 0.05$), using two-way analysis of variance. “a” indicates nanosubstrates that show statistically significant cell numbers w.r.t control substrates. “b”, “c” and “d” indicates nanosubstrates that show statistically significant cell numbers w.r.t 5 L, 10 L and 15 L nanosubstrates respectively.

2.3. Protein Assays

2.3.1. Bradford Assay

The total protein produced by fibrochondrocytes (FCs) on TiO₂ nanosubstrates and control substrates increased with the number of culture days and with an increase in the number of TiO₂ nanolayers. A substantial increase in FC functionality was observed with an increased in the number of layers of TiO₂ nanosubstrates as compared to control substrates (Figure 4). Statistical analyses on the Bradford assay indicated statistically significant ($p < 0.05$) FC functionality with an increase in culture days and with increasing nanothin film thickness.

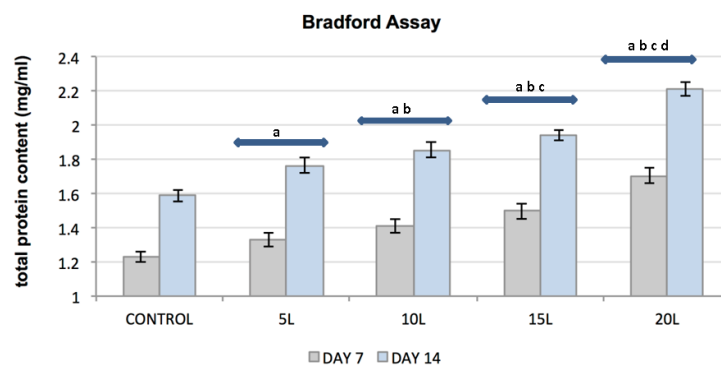


Figure 4. Plot represents FC total protein concentration (*y*-axis) as a function of control substrates and increasing nanolayers of TiO₂ nanosubstrates (*x*-axis) at 3, 7, 10 and 14 culture days. All data are shown as mean ± standard deviation, with a sample size of 6 for all substrates. Substrates represented by letters different (a, b, c, d) are considered statistically significant ($p < 0.05$), using two-way analysis of variance. “a” indicates nanosubstrates that show statistically significant cell numbers w.r.t control substrates. “b”, “c” and “d” indicates nanosubstrates that show statistically significant cell numbers w.r.t 5 L, 10 L and 15 L nanosubstrates respectively.

2.3.2. ELISA

ELISA was used to evaluate the effect of TiO₂ nanosubstrates and its increasing nanolayers on ECM protein expression. The increase in protein content was assessed at culture days 3, 7, 10 and 14. TiO₂ nanosubstrates and the control substrates supported the production of collagen types I and II and the proteoglycans decorin and aggrecan with increased protein production over the 14-day experimental period (Figures 5–8). Protein expression was substantially pronounced with increasing layers of TiO₂ nanosubstrates than control substrates. A prominent increase in collagen I was observed on the TiO₂ nanosubstrates followed by an increased production of decorin, aggrecan and collagen II. Statistical analysis indicated statistically significant ($p < 0.05$) ECM expression of the assessed proteins with increasing culture days and an increase in nanothin film thickness. With thicker nanofilms being a factor in promoting enhanced FC functionality, TiO₂ nanosubstrates could eventually aid in creating a potential scaffold mimicking the TMJ environment.

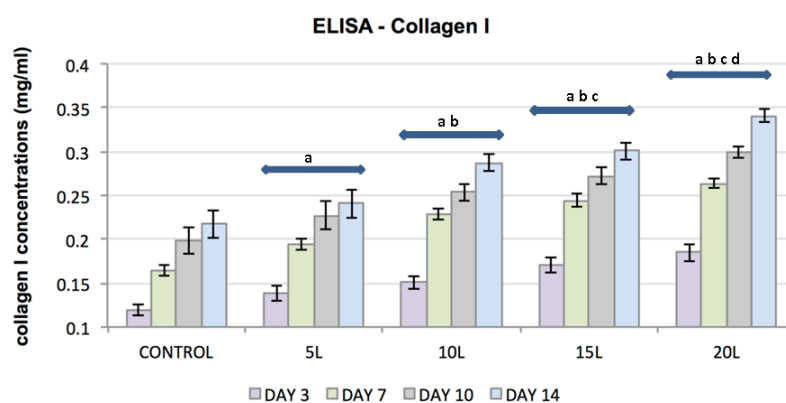


Figure 5. Plot represents FC collagen I concentration (y -axis) as a function of control substrates and increasing nanolayers of TiO₂ nanosubstrates (x -axis) at 3, 7, 10 and 14 culture days. All data are shown as mean \pm standard deviation, with a sample size of 6 for all substrates. Substrates represented by letters different (a, b, c, d) are considered statistically significant ($p < 0.05$), using two-way analysis of variance. “a” indicates nanosubstrates that show statistically significant cell numbers w.r.t control substrates. “b”, “c” and “d” indicates nanosubstrates that show statistically significant cell numbers w.r.t 5 L, 10 L and 15 L nanosubstrates respectively.

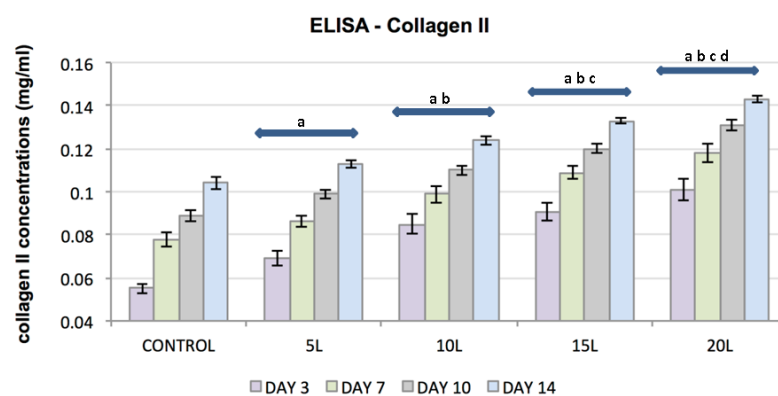


Figure 6. Plot represents FC collagen II concentration (y -axis) as a function of control substrates and increasing nanolayers of TiO₂ nanosubstrates (x -axis) at 3, 7, 10 and 14 culture days. All data are shown as mean \pm standard deviation, with a sample size of 6 for all substrates. Substrates represented by letters different (a, b, c, d) are considered statistically significant ($p < 0.05$), using two-way analysis of variance. “a” indicates nanosubstrates that show statistically significant cell numbers w.r.t control substrates. “b”, “c” and “d” indicates nanosubstrates that show statistically significant cell numbers w.r.t 5 L, 10 L and 15 L nanosubstrates respectively.

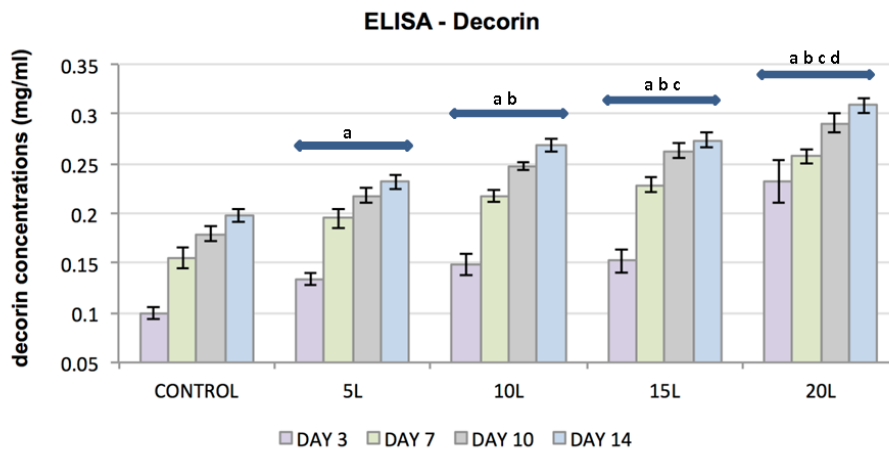


Figure 7. Plot represents FC decorin concentration (*y*-axis) as a function of control substrates and increasing nanolayers of TiO₂ nanosubstrates (*x*-axis) at 3, 7, 10 and 14 culture days. All data are shown as mean ± standard deviation, with a sample size of 6 for all substrates. Substrates represented by letters different (a, b, c, d) are considered statistically significant (*p* < 0.05), using two-way analysis of variance. “a” indicates nanosubstrates that show statistically significant cell numbers w.r.t control substrates. “b”, “c” and “d” indicates nanosubstrates that show statistically significant cell numbers w.r.t 5 L, 10 L and 15 L nanosubstrates respectively.

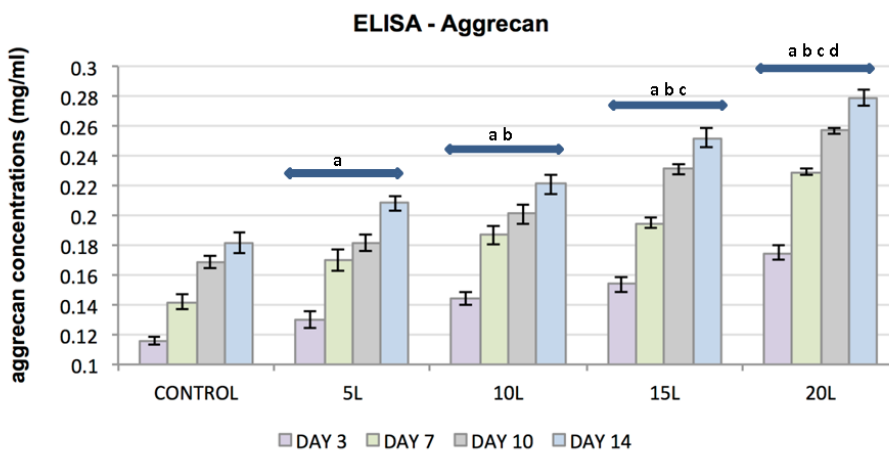


Figure 8. Plot represents FC aggrecan concentration (*y*-axis) as a function of control substrates and increasing nanolayers of TiO₂ nanosubstrates (*x*-axis) at 3, 7, 10 and 14 culture days. All data are shown as mean ± standard deviation, with a sample size of 6 for all substrates. Substrates represented by letters different (a, b, c, d) are considered statistically significant (*p* < 0.05), using two-way analysis of variance. “a” indicates nanosubstrates that show statistically significant cell numbers w.r.t control substrates. “b”, “c” and “d” indicates nanosubstrates that show statistically significant cell numbers w.r.t 5 L, 10 L and 15 L nanosubstrates respectively.

2.4. Statistical Significance

Two-way analysis of variance on the quantitative assays indicated higher statistical significance of FC proliferation and FC ECM markers, observed with increasing culture days and increased nanofilm thickness. Significant differences in the *F* value and *F*_{crit} value, with *F* > *F*_{crit}, was observed for culture days and the substrates employed, for the quantitative assays. Statistical analysis of the results suggests that increased TiO₂ nanofilm may be promoting an increase in FC proliferation resulting in enhanced FC functionality and an increase in specific markers of TMJ disc protein expression.

3. Discussion

The current study describes the first successful attempt to grow TMJ discal fibrochondrocytes on TiO₂ nanoparticle substrates prepared through LBL nanoassembly. Increasing TiO₂ nanofilm thickness was examined as a means for enhancing cell adhesion and functionality. Increase in cell proliferation with an increase in TiO₂ film thickness was observed, along with a stimulatory effect on protein synthesis. Enhanced protein synthesis on thicker TiO₂ nanosubstrates was evidenced by an increased expression in discal specific ECM proteins including collagen types I and II, aggrecan, and decorin. Synthesis of a fibrous matrix (type I collagen and decorin) predominated over a cartilaginous matrix (type II collagen and aggrecan), a pattern comparable to the native TMJ disc ECM where a fibrous matrix dominates over a localized cartilaginous matrix [1,2,4,8,17]. A stimulus towards FC proliferation may be seen as a positive outcome in that an increase in film thickness promoted cell growth but also provided a means for increased ECM synthesis.

LBL constructed TiO₂ nanofilms has shown prior success as a surface modification technique for bone implants [35,36]. Increasing TiO₂ film thickness was also linked to an enhanced osteoblastic and mesenchymal stem cell response [22,31,36,37]. Notably, in their conclusions, the authors pointed to an increase in TiO₂ film thickness and linked this with an increase in cell adhesion, proliferation, and matrix mineralization. A transitory shift from increased osteoblast proliferation to early matrix mineralization with thicker nanofilms was observed in a companion study, again demonstrating the importance of thicker TiO₂ nanofilms and cell functionality [35,37].

While our results are encouraging several factors still need to be investigated for the potential of LBL fabricated TiO₂ nanofilm for TMJ tissue repair, or regeneration may be recognized. What physical properties (surface roughness, hydrophilicity, porosity, or stiffness) of the TiO₂ nanosubstrates promoted protein synthesis over cell proliferation? Cell source and cell density have been widely recognized as a major challenge in TMJ bioengineering [17–19,38]. TMJ disc cells, articular chondrocytes, and costal chondrocytes have been studied extensively for use in bioengineering TMJ tissues [38,39]. However, many investigators have cited the lack of clinical translatability of these cells for engineering new discal and mandibular condyle tissues [17–19,38,39]. Control over phenotype was also an issue identified in several studies using various types of TMJ cells. In many discal constructs generated, the seeded cells developed a more chondrocytic phenotype, with a rounded morphology, and positive staining for aggrecan and type II collagen and an overall matrix with more hyaline-like cartilage characteristics [39–43]. Recently, costal chondrocytes have showed promise as a cell source [44–46]. It was demonstrated that costal chondrocyte scaffold-less constructs could be generated with cellularity and a glycosaminoglycan content significantly greater than the disc-cell constructs, with retention of overall size and shape [44,45]. Stem cells have also emerged as a promising cell source for mandibular condyle tissue regeneration, although more investigation is required before their medical potential can be fully known [46–48].

This study and others have shown that TiO₂ nanofilms support fibroblast, chondroblast, osteoblast, and mesenchymal stem cell growth and permit synthesis of an appropriate tissue matrix [22,31–33,35–38]. TiO₂ films can be formed on many surfaces and polymers including poly(lactide), polycaprolactone, and poly(D,L lactic acid) (PDLLA) [49–51] and modulated for the desired surface characteristics. Gerhardt *et al.* (2007), for example, used TiO₂ nanoparticles to create a nanometer surface topography and to enhance roughness on PDLLA for bone tissue engineering [52].

Further control over matrix production by FCs might be obtained with embedded drugs, growth factors or proteins used as biological signaling agents [30,32,40,41]. The role of an instructional agent such as BMP-2 or TGF- β or the synergistic effect of different instructional agents at their effective dosage may be a means to support a regulated increase in ECM synthesis on TiO₂ nanofilms. In addition, the potential additive role of biomechanical stimuli and its effects on nanofilm integrity and longevity need to be investigated. Accordingly, TiO₂ LBL nanofilms could be custom tailored to the biological requirements of a range of TMJ tissues including bone, cartilage, ligaments, and tendon according to the cell and tissue requirements of the affected area.

The past successes of LBL fabricated TiO₂ nanothin films indicate the potential of this novel technique in contributing critical features to a scaffolding material for TMJ disc reconstruction or repair. Although finding an ideal TMJ discal scaffold for repair or regeneration remains a critical challenge, the current study on TiO₂ nanofilms, suggests it may have potential as a TMJ scaffolding material.

4. Materials and Methods

4.1. Fibrochondrocyte Isolation and Maintenance

TMJ discs extracted from sacrificed bovine heads (CKC Farms, Pitkin, LA, USA) were employed in isolating FCs. Complete Dulbecco's Modified Eagle Medium (DMEM) (Biosource, Rockville, MD, USA) was used in culturing the obtained cells and, consisted 500 mL of DMEM supplemented with 10% FBS (Fetal Bovine Serum) (Biosource, Rockville, MD, USA), 10 µg/mL ascorbic acid (Sigma, St. Louis, MO, USA), and 5% penicillin-streptomycin-fungizone (PenStrep). Prior to tissue dissociation, the discs were sterilized with a thorough rinse in 3X Hank's Balanced Salt Solution (HBSS) (Biosource, Rockville, MD, USA) supplemented with 1X PenStrep (Biosource, Rockville, MD, USA), followed with a 24-hour incubation in complete DMEM to which 5X PenStrep was added. Enzymatic digestion of the disc with collagenase (Biosource, Rockville, MD, USA) and pronase (Biosource, Rockville, MD, USA) and, mechanical stirring of the tissue digest released FCs. FCs were then plated in 60 mm tissue culture plastic (TCP) (Biosource, Rockville, MD, USA) at an appropriate density. The cells were maintained in complete DMEM in a humidified environment at 37 °C, 5% CO₂ and 95% air. Until a required confluence was obtained, the media was replaced every 24 h after initial cellular attachment. Fibrochondrocytes were passaged twice to obtain an appropriate density of cells for the quantitative analyses.

4.2. TiO₂ LBL Nanothin Film Formation

An automated robotic dipping machine (manufactured by Riegler and Kirstein GmbH, Potsdam, Germany), was used in the preparation of nanoscale substrates for mass production and uniformity in film deposition. Sterile, hydrophilic glass substrates were used as control substrates and, for the deposition of nanothin films via the LBL fabrication technique. Precleaned glass substrates were sterilized with ultrasonication in 50% isopropanol, overnight immersion in 75% ethanol solution, thorough rinse with DI followed by drying the glass substrates with a nitrogen gas stream. The nanometer- thick thin films were formed on sterile glass substrates via the conventional dipping technique. Nanosubstrates consisted of 3 alternating layers of Poly (styrene sulfonate) sodium salt (PSS, MW ~ 70 kDa, Sigma, Polyanion) and Poly (dimethyldiallyl ammonium chloride) (PDDA, MW ~ 200 kDa, Sigma, Polycation), with a thickness of about 10nm as precursor layers, onto which active layers were deposited for uniformity and better adhesion. Cationic TiO₂ nanoparticles (diameter ~21 nm, Aeroxide TiO₂, P25 Degussa AG, Mari, Germany) used in alternation with anionic PSS formed the active layers, with TiO₂ being the terminating layer in all cases. (Complete details on TiO₂ nanofilms assembly and component preparation are mentioned in reference [31]). TiO₂ nanosubstrates (5,10,15 and 20-layered) were prepared and evaluated for FC response.

4.3. Fibrochondrocyte Seeding on TiO₂ Nanosubstrates and Control Substrates

Nanosubstrates and control substrates were sterilized with its' overnight immersion in 75% alcohol and a thorough rinse in HBSS, before FC seeding was ensued. FC's at a density of about 5000 cells/cm² were then plated and the seeded substrates were placed in 24 well plates containing complete DMEM and, were maintained in a humidified environment at 37 °C, 5% CO₂ and 95% air for cellular attachment and confluence. Quantitative analyses and viability studies were then performed on FC seeded substrates and FC response was evaluated at different culture period.

4.4. Live Dead Cytotoxicity Assay

The viability studies were performed using a Live/Dead Cell cytotoxicity assay (Biovision, Milpitas, CA, USA). The kit contains Live-Dye™ a cell-permeable green fluorescent dye ($E_x/E_m = 488/518$ nm), to stain live cells in green, and propidium iodide (PI), a cell non-permeable red fluorescent dye ($E_x/E_m = 488/615$), to stain dead cells in yellow-red. For viability studies, staining solution was prepared by mixing 1 μ L of solution A (1 mM Live-Dye) and 1 μ L of solution B (2.5 mg/mL PI) to 1 mL of Staining Buffer. The seeded substrates were washed twice with HBSS and then 150 μ L of staining solution was added to each substrate. These substrates were then incubated at 37 °C for 15 min. Slides were assessed for cell viability and observed on day 7, 14, and 21 using an Olympus BX51 epifluorescent microscope and representative images were captured using a Nikon digital camera.

4.5. Proliferation Assays

4.5.1. MTT Proliferation Assay

The MTT assay determined FC proliferative rate on different layered (5,10,15 and 20) TiO₂ nanosubstrates and control substrates at 7 and 14 culture days. The principle of the assay is based on the reduction of yellow tetrazolium MTT, 3-[4,5-dimethylthiazol-2-yl]-2,5-diphenyl-tetrazolium bromide, to purple formazan crystals that indicated cellular mitochondrial activity and thus proliferating cell densities in a given culture. FC seeded substrates were rinsed with HBSS free of phenol red and incubated with MTT working solution, at the end of the culture period. The substrates were incubated for about 4 h in a CO₂ incubator at 37 °C, at a volume that was 10% of the volume of media (complete DMEM). Interaction of mitochondrial dehydrogenase enzyme present in the metabolically active viable cells with the yellow MTT generated reducing equivalents NADH and NADPH that yielded intracellular purple formazan crystals on the surface of the substrates at the end of the incubation period. The crystals were then solubilized using acidified isopropanol and quantified for FC proliferation. Spectrophotometric quantification of proliferating FC's on the substrates' surface (at a wavelength of 570 nm and a reference wavelength of 690 nm) and, the linear relationship established between FC densities and the corresponding absorbance measurements (graph not given) enabled the accurate quantification of the proliferating FC densities. Six samples were considered for each type of substrate and for all assays to obtain accurate readings.

4.5.2. DNA Quantitation Assay

DNA assay was used to test the accuracy and reliability of the MTT results. In our hands, the MTT assay often provides results that may be incorrectly interpreted. The assay assessed the proliferative activity of FCs on different layered (5, 10, 15 and 20) TiO₂ nanosubstrates and control substrates at culture period of 3, 7, 10 and 14 days. The principle of the assay is based on detecting the amount of dsDNA produced during the S phase with an ultrasensitive fluorescent nucleic acid stain, Picogreen reagent, indicating the number of dividing cells during mitosis. A standard DNA curve (graph not given) established between different FC densities and fluorescing dsDNA samples enabled to obtain the number of proliferating cells from the fluorescing samples at an excitation wavelength of 485 nm and emission wavelength of 535 nm. Six samples were considered for each type of substrate and for all assays to obtain accurate readings.

4.6. Protein Assays

4.6.1. Bradford Assay

Bradford assay quantified the total protein content produced by different layered (5, 10, 15 and 20) TiO₂ nanosubstrates and control substrates at 7 and 14 culture days. The assay essentially made use of Bradford dye, Coomassie®R Brilliant Blue G-250, which exhibited differential color change on

binding to various concentrations of protein present in the given samples. Absorbance from the dye-binding calorimetric reaction was measured spectrophotometrically at a wavelength of 595 nm and, the total protein content was quantified from the standard protein curve established between different concentrations of Bovine Serum Albumin (BSA) and the corresponding absorbance measurements at different BSA concentrations.

4.6.2. ELISA

The biosynthetic activity of TiO₂ nanosubstrates and control substrates were realized with the expression of type I and type II collagen, aggrecan and decorin, the significant TMJ ECM phenotype markers. ELISA was used to detect the specific ECM protein production on different layered (5, 10, 15 and 20) TiO₂ nanosubstrates and control substrates at culture period of 3, 7, 10 and 14 days. A suite of anti-cartilage matrix monoclonal antibodies was used in the calorimetric detection of the antigens of interest. The primary antibodies used for collagen I (M-38), collagen II (CIICI) and decorin (DS1) were purchased from the Developmental Hybridoma Labs, University of Iowa, Iowa City, IA, USA. The primary antibody used for aggrecan (1R11) was obtained from (Invitrogen-Molecular Probes, Grand Island, NY, USA). The cascade of antigen-antibody complexes formed was identified by the peroxidase anti-peroxidase method (VECTASTAIN Elite ABC Kit-mouse Vector Laboratories, Burlingame, CA, USA), catalyzed by alkaline phosphatase and, was converted into a detectable signal in the presence of a chromogenic substrate like pNPP. Absorbance was then measured from the resulting calorimetric reactions at a wavelength of 405 nm. The amount of specific antigen present in the samples was then determined by the linear relationship (standard curve not available in the given article) established between different antibody concentrations and the corresponding absorbance measurements.

4.7. Statistical Analysis

Quantitative analyses of fibrochondrocyte proliferation and functionality were analyzed using two-way analysis of variance (ANOVA) with statistical significance set at $p < 0.05$. Values are expressed as mean \pm SD ($n = 6$).

5. Conclusions

TiO₂ nanoparticle thin films were assembled through LbL nanoassembly. Temporomandibular joint fibrochondrocytes thrived on these substrates and maintained their phenotype and functionality on TiO₂ nanofilms. An increase in the number TiO₂ nanofilm bilayers was shown to enhanced fibrochondrocyte cell behavior. While this study focused on fibrochondrocytes, we believe other cell types, such as chondroblasts, osteoblasts and mesenchymal stem cells will also grow and maintain functionality on these nanoparticle nanofilms.

Acknowledgments: The authors would like to thank the funding support of the Louisiana Governor's Biotechnology Fund.

Author Contributions: Sharon Ronald and David K. Mills conceived and designed the experiments; Sharon Ronald performed the experiments; Sharon Ronald and David K. Mills analyzed the data; Sharon Ronald and David K. Mills wrote the paper.

Conflicts of Interest: The authors declare no conflict of interest.

References

1. Kalpakci, K.N.; Willard, V.P.; Athanasiou, K.A. An interspecies comparison of the temporomandibular joint disc. *J. Dent. Res.* **2011**, *90*, 190–198. [[CrossRef](#)] [[PubMed](#)]
2. Mills, D.K.; Fiandaca, D.J.; Scapino, R.P. Morphologic, microscopic and immunohistochemical investigations into the function of the primate TMJ disc. *J. Orofac. Pain* **1994**, *8*, 136–154. [[PubMed](#)]
3. Milam, S.B. Pathophysiology and Epidemiology of TMJ. *J. Musculoskelet. Neuronal Interact.* **2003**, *3*, 382–390. [[PubMed](#)]

4. Mills, D.K.; Daniel, J.C.; Scapino, R.P. Histological features and *in vitro* proteoglycan synthesis in the rabbit craniomandibular joint disc. *Arch Oral Biol.* **1988**, *33*, 195–202. [[CrossRef](#)]
5. Berkovitz, B.K.; Robertshaw, H. Ultrastructural quantification of collagen in the articular disc of the temporomandibular joint of the rabbit. *Arch Oral Biol.* **1993**, *38*, 91–95. [[CrossRef](#)]
6. Scapino, R.P.; Canham, P.; Finlay, H.M.; Mills, D.K. The behavior of collagen fibers in stress relaxation and stress distribution in the jaw joint disc of rabbits. *Arch Oral Biol.* **1996**, *41*, 1039–1052. [[CrossRef](#)]
7. Taguchi, N.; Nakata, S.; Oka, T. Three-dimensional observation of the temporomandibular joint disk in the rhesus monkey. *J. Oral Surg.* **1980**, *38*, 11–15. [[PubMed](#)]
8. Milam, S.B.; Klebe, R.J.; Triplett, R.G.; Herbert, D. Characterization of the extracellular matrix of the primate temporomandibular joint. *J. Oral Maxillofac. Surg.* **1991**, *49*, 381–391. [[CrossRef](#)]
9. Fujita, S.; Hoshino, K. Histochemical and immunohistochemical studies on the articular disk of the temporomandibular joint in rats. *Acta Anat (Basel)* **1989**, *134*, 26–30. [[CrossRef](#)] [[PubMed](#)]
10. Mathema, A.; Mills, D.K. Effects of mechanical shear on anisotropic tissue engineered construct as potential TMJ repair material. *FASEB J.* **2012**, *26*, 729.
11. Allen, K.D.; Athanasiou, K.K. Effect of Passage and Topography on Gene Expression on Temporomandibular Joint Disc Cells. *Tissue Eng.* **2007**, *13*, 101–110. [[CrossRef](#)] [[PubMed](#)]
12. Mills, D.K.; Daniel, J.C.; Herzog, S.; Scapino, R.P. An animal model for studying mechanisms in human temporomandibular joint disc derangement. *J Oral Maxillofac. Surg.* **1994**, *52*, 1279–1292. [[CrossRef](#)]
13. Tanaka, E.; Detamore, M.S.; Mercuri, L.G. Degenerative disorders of the temporomandibular joint, etiology, diagnosis, and treatment. *J. Dent. Res.* **2008**, *87*, 296–307. [[CrossRef](#)] [[PubMed](#)]
14. Ingawaleal, S.; Goswami, T. Temporomandibular joint, disorders, treatments, and biomechanics. *Ann. Biomed. Eng.* **2009**, *37*, 976–996. [[CrossRef](#)] [[PubMed](#)]
15. Baskan, S.; Zengingul, A. Temporomandibular joint: Disorders and approaches. *Biotech. Biotechnol.* **2006**, *20*, 151–155. [[CrossRef](#)]
16. Baird, D.N.; Rea, W.N. The temporomandibular joint implant controversy: A review of autogeneous alloplastic materials and their complications. *J. Nutr. Environ. Med.* **1998**, *8*, 289–300.
17. Willard, V.P.; Zhang, L.; Athanasiou, K.A. Tissue engineering of the temporomandibular joint. In *Comprehensive Biomaterials*, 1st ed.; Ducheyne, D., Healy, K., Hutmacher, D., Kirkpatrick, J., Eds.; Elsevier: London, UK, 2010; pp. 222–234.
18. Detamore, M.S.; Athanasiou, K.A. Motivation, characterization, and strategy for tissue engineering the temporomandibular joint disc. *Tissue Eng.* **2003**, *9*, 1065–1087. [[CrossRef](#)] [[PubMed](#)]
19. Murphy, M.K.; Murphy, M.K.; Masters, T.E.; Hu, J.C.; Athanasiou, K.A. Engineering a fibrocartilage spectrum through modulation of aggregate redifferentiation. *Cell Trans.* **2014**, *24*, 235–245. [[CrossRef](#)] [[PubMed](#)]
20. Allen, K.D.; Athanasiou, K.A. Scaffold and growth factor selection in temporomandibular joint disc engineering. *J. Dent. Res.* **2008**, *87*, 180–185. [[CrossRef](#)] [[PubMed](#)]
21. Webster, T. Nanostructured surface roughness for the control of protein and cell functions. In *Handbook of Nanostructured Biomaterials and Their Applications in Nanobiotechnology*; Nalwa, H.S., Ed.; American Scientific Publishers: Stevenson Ranch, CA, USA, 2005; Volume 1.
22. Kommireddy, D.S.; Patel, A.A.; Shutava, G.; Mills, D.K.; Lvov, Y. Layer-by-layer assembly of TiO₂ nanoparticles for stable hydrophilic biocompatible coatings. *J. Nanosci. Nanotech.* **2005**, *5*, 1081–1087. [[CrossRef](#)]
23. Ben-Nissan, B. *Biomedical Thin Films: Mechanical Properties*, 1st ed.; Ducheyne, D., Healy, K., Hutmacher, D., Kirkpatrick, J., Eds.; Elsevier: London, UK, 2010; pp. 63–82.
24. Zhu, X.; Chen, J.; Scheideler, L.; Reichl, R.; Geis-Gerstorfer, J. Effects of topography and composition of titanium surface oxides on osteoblast responses. *Biomaterials* **2004**, *25*, 4087–4103. [[CrossRef](#)] [[PubMed](#)]
25. Nayab, S.N.; Jones, F.H.; Olsen, I. Effects of calcium ion implantation on human bone cell interaction with titanium. *Biomaterials* **2005**, *26*, 4717–4727. [[CrossRef](#)] [[PubMed](#)]
26. Schuler, M.; Trentin, D.; Textor, M.; Tosatti, S.G. Biomedical interfaces, titanium surface technology for implants and cell carriers. *Nanomed* **2006**, *1*, 449–463. [[CrossRef](#)] [[PubMed](#)]
27. Heimke, G.; Wittal, D.L. Osteointegrated Dental Implants. In *Orthopedic, Dental and Bone Graft Applications*; Wise, D.L., Trantolo, D.J., Lewandrowski, K., Gresser, J.D., Cattaneo, M.V., Yaszemski, M.J., Eds.; Humana Press: Totowa, NJ, USA, 2000; Volume 1, pp. 67–92.

28. Torrecillas, R.; Moya, J.S.; Diaz, L.A.; Bartolome, J.F.; Fernandez, A.; Lopez-Esteban, S. Nanotechnology in joint replacement. *Nanomed. Nanobiotech.* **2009**, *1*, 540–552. [[CrossRef](#)] [[PubMed](#)]
29. Abdllayev, E.; Lvov, Y. Functional polymer clay nanotube composites with sustained release of chemical agents. *Prog. Poly. Sci.* **2013**, *38*, 1690–1719.
30. Leguen, E.; Chassepot, A.; Decher, G.; Schaaf, P.; Voegel, J.; Jessel, N. Bioactive coatings based on polyelectrolyte multilayer architectures functionalized by embedded proteins, peptides or drugs. *Biomol. Eng.* **2007**, *24*, 33–41. [[CrossRef](#)] [[PubMed](#)]
31. Kommireddy, D.S.; Lvov, Y.; Mills, D.K. Nanoparticle thin films, surface modification for cell attachment and growth. *Biomed. Nanotech.* **2005**, *1*, 286–290. [[CrossRef](#)]
32. Jessel, N.; Atalar, F.; Lavalle, J.; Mutterer, G.; Decher, G.; Schaaf, J.; Voegel, J.; Ogier, J. Bioactive coatings based on a polyelectrolyte multilayer architecture functionalized by embedded proteins. *Adv. Mat.* **2003**, *15*, 692–695. [[CrossRef](#)]
33. Zhu, H.; Ji, J.; Shen, J. Osteoblast growth promotion by protein electrostatic self assembly on biodegradable poly(lactide). *J. Biomat. Sci.* **2005**, *16*, 761–774. [[CrossRef](#)]
34. Guillot, R.; Gilde, F.; Becquart, P.; Sailhan, F. The stability of BMP loaded polyelectrolyte multilayer coatings on titanium. *Biomaterials* **2013**, *34*, 5737–5746. [[CrossRef](#)] [[PubMed](#)]
35. Sriram, S.M. Mesenchymal stem cell behavior and osteogenic differentiation on layer-by-layer assembled nanoparticle thin films. Master Thesis, Louisiana Tech University, Ruston, LA, USA, 2006.
36. Kommireddy, D.S.; Sriram, S.M.; Lvov, Y.; Mills, D.K. Stem cell attachment to layer-by-layer assembled TiO₂ nanoparticle thin films. *Biomaterials* **2006**, *27*, 4296–4303. [[CrossRef](#)] [[PubMed](#)]
37. Chenna, S.G. The Influence of Nanoparticle Thin Films on the Behavior of Osteoblast Cells *in vitro*. Master Thesis, Louisiana Tech University, Ruston, LA, USA, 2006.
38. Murphy, M.K.; Macbarb, R.F.; Wong, M.E.; Athanasiou, K. A Temporomandibular joint disorders: A review of etiology, clinical management, and tissue engineering strategies. *Int. J. Oral Maxillofac. Implants* **2013**, *28*, e393–e414. [[CrossRef](#)] [[PubMed](#)]
39. Johns, D.E.; Wong, M.E.; Athanasiou, K.A. Clinically relevant cell sources for TMJ disc engineering. *J. Dent Res.* **2008**, *87*, 548–552. [[CrossRef](#)] [[PubMed](#)]
40. Thomas, M.; Grande, D.; Haug, R.H. Development of an *in vitro* temporomandibular joint cartilage analog. *J. Oral Maxillofac. Surg.* **1991**, *49*, 854–856. [[CrossRef](#)]
41. Puelacher, W.C.; Wisser, J.; Vacanti, C.A.; Ferraro, N.F.; Jaramillo, D.; Vacanti, J.P. Temporomandibular joint disc replacement made by tissue-engineered growth of cartilage. *J. Oral Maxillofac. Surg.* **1994**, *52*, 1172–1177. [[CrossRef](#)]
42. Springer, I.N.; Fleiner, B.; Jepsen, S.; Acil, Y. Culture of cells gained from temporomandibular joint cartilage on non-absorbable scaffolds. *Biomaterials* **2001**, *22*, 2569–2577. [[CrossRef](#)]
43. Almarza, A.J.; Athanasiou, K.A. Seeding techniques and scaffolding choice for tissue engineering of the temporomandibular joint disk. *Tissue Eng.* **2004**, *10*, 1787–1095. [[CrossRef](#)] [[PubMed](#)]
44. Anderson, D.E.; Athanasiou, K.A. Passaged goat costal chondrocytes provide a feasible cell source for temporomandibular joint tissue engineering. *Ann. Biomed. Eng.* **2008**, *36*, 1992–2001. [[CrossRef](#)] [[PubMed](#)]
45. Anderson, D.E.; Athanasiou, K.A. A comparison of primary and passaged chondrocytes for use in engineering the temporomandibular joint. *Arch Oral Biol.* **2009**, *54*, 138–145. [[CrossRef](#)] [[PubMed](#)]
46. Johns, D.E.; Athanasiou, K.A. Growth factor effects on costal chondrocytes for tissue engineering fibrocartilage. *Cell Tissue Res.* **2008**, *333*, 439–447. [[CrossRef](#)] [[PubMed](#)]
47. Willard, V.P. Characterization of the Temporomandibular Joint Disc and Fibrocartilage Engineering using Human Embryonic Stem Cells. Ph.D. Thesis, Rice University, Houston, TX, USA, 2012.
48. Zhang, S.; Yap, A.U.; Toh, W.S. Stem cells for temporomandibular joint repair. *Stem Cell Rev.* **2015**, *11*, 728–742. [[CrossRef](#)] [[PubMed](#)]
49. Buzarovska, A. PLA nanocomposites with functionalized TiO₂ nanoparticles. *Poly.-Plast. Technol. Eng.* **2013**, *52*, 280–286. [[CrossRef](#)]
50. Ghosal, K.; Thomas, S.; Kalarikkal, N.; Gnanamani, A. Collagen coated electrospun polycaprolactone (PCL) with titanium dioxide (TiO₂) from an environmentally benign solvent, preliminary physico-chemical studies for skin substitute. *J. Poly. Res.* **2014**, *21*, 410–415. [[CrossRef](#)]

51. Boccaccini, A.R.; Blaker, J.J.; Maquet, M.; Chung, W.; Jerome, R.; Nazhat, S.N. Poly(DL-lactide) (PDLA) foams with TiO₂ nanoparticles and PDLA/TiO₂-bioglass[®] foam composites for tissue engineering scaffolds. *J. Mat. Sci.* **2006**, *41*, 3999–4008. [[CrossRef](#)]
52. Gerhardt, L.C.; Jell, A.G.M.; Boccaccini, A.R. Titanium dioxide (TiO₂) nanoparticles filled poly(D,L lactid acid) (PDLA) matrix composites for bone tissue engineering. *J. Mater. Sci. Mater. Med.* **2007**, *18*, 1287–1298. [[CrossRef](#)] [[PubMed](#)]



© 2016 by the authors; licensee MDPI, Basel, Switzerland. This article is an open access article distributed under the terms and conditions of the Creative Commons Attribution (CC-BY) license (<http://creativecommons.org/licenses/by/4.0/>).